

# Water Resources Research



#### RESEARCH ARTICLE

10.1029/2022WR034168

#### **Key Points:**

- Simulation of water age with a validated hydrodynamic model against temperature and currents
- Average water age (surrogate to residence time) in bays is smaller than 6 days
- Spatial distribution of water age within bays is not uniform and strong wind events lead to lower water age within 1 day

#### **Supporting Information:**

Supporting Information may be found in the online version of this article.

#### Correspondence to:

G. A. R. Auger, guillaume.auger@ibm.com

#### Citation:

Auger, G. A. R., Kelly, M. R., Moriarty, V. W., Rose, K. C., & Kolar, H. R. (2024). Understanding lake residence time across spatial and temporal scales: A modeling analysis of Lake George, New York USA. *Water Resources Research*, 60, e2022WR034168. https://doi.org/10.1029/2022WR034168

Received 23 NOV 2022 Accepted 8 JAN 2024

#### **Author Contributions:**

Conceptualization: Guillaume A. R. Auger, Michael R. Kelly, Vincent W. Moriarty, Kevin C. Rose, Harry R. Kolar Data curation: Guillaume A. R. Auger, Michael R. Kelly, Vincent W. Moriarty Formal analysis: Guillaume A. R. Auger Investigation: Guillaume A. R. Auger Methodology: Guillaume A. R. Auger, Kevin C. Rose

Resources: Harry R. Kolar Validation: Guillaume A. R. Auger Visualization: Guillaume A. R. Auger

© 2024 IBM Research and The Authors. This is an open access article under the terms of the Creative Commons Attribution-NonCommercial-NoDerivs License, which permits use and distribution in any medium, provided the original work is properly cited, the use is non-commercial and no modifications or adaptations are made.

## Understanding Lake Residence Time Across Spatial and Temporal Scales: A Modeling Analysis of Lake George, New York USA

Guillaume A. R. Auger<sup>1</sup>, Michael R. Kelly<sup>1,2</sup>, Vincent W. Moriarty<sup>1,2</sup>, Kevin C. Rose<sup>2</sup>, and Harry R. Kolar<sup>1</sup>

<sup>1</sup>IBM Research, Yorktown Heights, NY, USA, <sup>2</sup>Rensselaer Polytechnic Institute, Troy, NY, USA

Abstract Whole lake residence time has been associated with various water quality parameters, including harmful algal blooms. Despite observations of spatial variability in commonly measured lake water quality parameters, little attention is given to the spatial variability of residence time in lakes. In this paper we use water age as a surrogate for residence time and we examine its spatial and temporal distribution in 10 bays of varying size in Lake George, New York (USA). Using a validated hydrodynamic model against observations of water temperature and water currents, and using simulated water age, we show that the average residence time in most of the bays is less than 3 days. Timeseries of bay-average water age shows that it can sharply decrease within 1 day due to a strong wind event. The average spatial distribution is shown to be non-uniform, with only a small section of the bottom layer of the bays having a substantially greater age, which may be more than 1 week in certain bays. Snapshots of water age transects indicate that strong wind events substantially change the vertical distribution of water age in some bays, even to the extent of inverting the distribution. The substantial decreases of water age in the bays were associated with the shallowing and deepening of the thermocline. Our results highlight how variations in water residence times within lakes could introduce substantial variation in water quality attributes. Whole lake residence times may serve as a poor proxy to understand the dynamics of water masses, especially in large and morphologically complex waterbodies.

#### 1. Introduction

Lentic ecosystems such as lakes and ponds are often conceptualized as homogenous and quiescent bodies of water. Indeed, the term *lentic* derives from the Latin *lentus*, meaning slow or motionless (Marsh & Fairbridge, 1999). However, the reality is that lakes are dynamic, heterogenous ecosystems. The mean time water spends in a lake, or residence time, is a key attribute regulating many aspects of aquatic ecosystem heterogeneity. For example, increases in residence times have been associated with relatively large algal blooms (Michalak et al., 2013; Zhao et al., 2022). Residence time also controls biogeochemical functioning. For example (Evans et al., 2017), noted that inland waterbodies with low water residence time were biogeochemical hotspots for the processing of dissolved organic carbon.

Because spatial variability is frequently correlated with temporal variability (Rose et al., 2017) understanding lake spatial heterogeneity may be aided by improving assessments of residence times at the sub-basin scale. If a waterbody is composed of a main basin surrounded by embayments, the mean residence time would largely reflect the residence time of the main basin due to its volume. However, the residence time of the bays will not necessarily be the same as the main basin of the lake. Their residence times may be highly variable both across sites and through time, depending on factors such as weather patterns, seasonality, and basin exchange rates and the scaling relationship between residence time and water volume is poorly constrained.

The residence times of most lakes is relatively short, highlighting the dynamic nature of most waterbodies. For example, in one analysis of 45,000 US waterbodies, 75% of residence times were under 1 year (Fergus et al., 2020). A separate analysis showed that 50% of residence times of US lakes were under 0.52 years, with variance in residence time associated with lake depth and watershed size (Brooks et al., 2014). Within lakes, the residence time of particular sub-basins or depth layers (e.g., during the stratified season) is likely to be much shorter, however, residence times at the sub-basin scale may also demonstrate high spatial variability, especially in larger lakes.

AUGER ET AL. 1 of 17



## **Water Resources Research**

10.1029/2022WR034168

Writing – original draft: Guillaume A. R. Auger Writing – review & editing: Guillaume A. R. Auger, Michael R. Kelly, Vincent W. Moriarty, Kevin C. Rose, Harry R. Kolar

Another useful measure associated with residence time is water age, which indicates the average time the water has remained in the volume at time *t*. Conceptually, mean residence time is the upper range of water age (Rueda & Cowen, 2005), however, water age often has a similar value to residence time. Rayson et al. (2016) compared simulated water age against residence time and found similarities in their spatial distribution and the temporal changes between the two timescales. Their results corroborate Duffy et al. (2018)'s use of water age as a surrogate to residence time. Similar to sub-basin residence times, the spatial distribution of water age is far from homogeneous. For example, in a simulation of Lake Mead, Li et al. (2010) found several locations had water with estimated ages of 100 days or greater. However, a change in water inflow led to a substantial decrease in the vertically averaged water age, by 80 days on average. Separately, Liu et al. (2020) found that a change in wind direction led to changes in both the average value and horizontal pattern of water age in Taihu Lake (China). Their results allude to the importance of meteorological forcing on the spatial variability of water age within a lake.

Here, we investigate Lake George, a large oligotrophic lake located in the Adirondack Park, New York, US. Lake George has experienced declines in some water quality parameters (Hintz et al., 2020). They reported an increase in chloride concentration due to road deicing salts, but also an increase of orthophosphate and chlorophyll-a concentrations in the epilimnion over the last several decades. More recently, blooms of *dolichopsermum*, with toxin concentrations below detection levels, were observed since October 2020 (NYDEC, 2022) on the shore and within some of the bays of Lake George. Swinton and Boylen (2014) reported an increase of chlorophyll-a in Northwest Bay in Lake George after an intense rain event. It is important to understand the dynamics in the bays and how quickly elements are redistributed from the bays to the main basin of the lake, however, the dynamics in the bays of Lake George remain under-addressed. We used mean water age as a surrogate to residence time and we investigated its dynamics within multiple embayments in Lake George, NY. By understanding transport rates, residence times, and water ages across sites and varying spatial scales, our results improve the understanding of the underlying sources of ecological heterogeneity that exist in large, complex aquatic ecosystems. Using Lake George as an archetypal site, our results demonstrate that residence times and water ages can vary over orders of magnitude across sites and through time. This variability introduces a key source of ecological heterogeneity across time and space, challenging the traditional paradigm of lakes as quiescent or well-mixed ecosystems.

#### 2. Methods

#### 2.1. Study Site

We focused our study on Lake George, NY (USA). Lake George is located in the Adirondack State Park and is composed of two basins linked by a narrow section with approximately 180 islands known as The Narrows. The lake is 55 km long, 2 km wide on average, and has average and maximum depths of 20 and 54 m, respectively. Lake George is located 98 m above sea level and is surrounded by the Adirondack Mountain Range that reaches more than 700 m above sea level.

We deployed two robotic vertical profiler buoys, each equipped with YSI EXO2 multiparameter sondes to measure water temperature over depth and time, in the south basin of Lake George. We also deployed terrestrial weather stations at multiple shoreline locations, on two rock outcroppings within the lake, and on the vertical profilers. We used these data to parameterize and validate a lake hydrodynamic model, which we used to characterize spatial and temporal variations in lake water residence time in 10 bays of Lake George, NY.

#### 2.2. Available Observations

In 2022, we deployed two vertical profilers in Lake George, both in the south basin. The more southern vertical profiler was deployed near Tea Island and the second vertical profiler was deployed in Harris Bay. Hereafter, we refer to the profiler at Tea Island as TI profiler and HB profiler for the profiler moored in Harris Bay. The TI profiler was deployed on 18 May 2022 and collected water temperature profiles to a depth of 28 m with a vertical resolution of 1 m on an hourly basis. The HB station was deployed on 22 April 2022, and collected water temperature profiles to a depth of 11 m at a vertical resolution of 0.5 m every 30 min. We direct the reader to Figure 1a for the locations of the profilers in Lake George.

Starting 20 May 2022, the vertical profiler at Harris Bay station sampled water current profiles with a downward-looking 600 kHz Workhorse Acoustic Doppler Current Profiler (ADCP; Teledyne RD Instruments) at

AUGER ET AL. 2 of 17

19447973, 2024, 2, Downloaded from https://agupubs.onlinelibrary.wiley.com/doi/10.1029/2022WR034168 by Rensselaer Polytechnic Institute, Wiley Online Library on [04/04/2024]. See the Terms

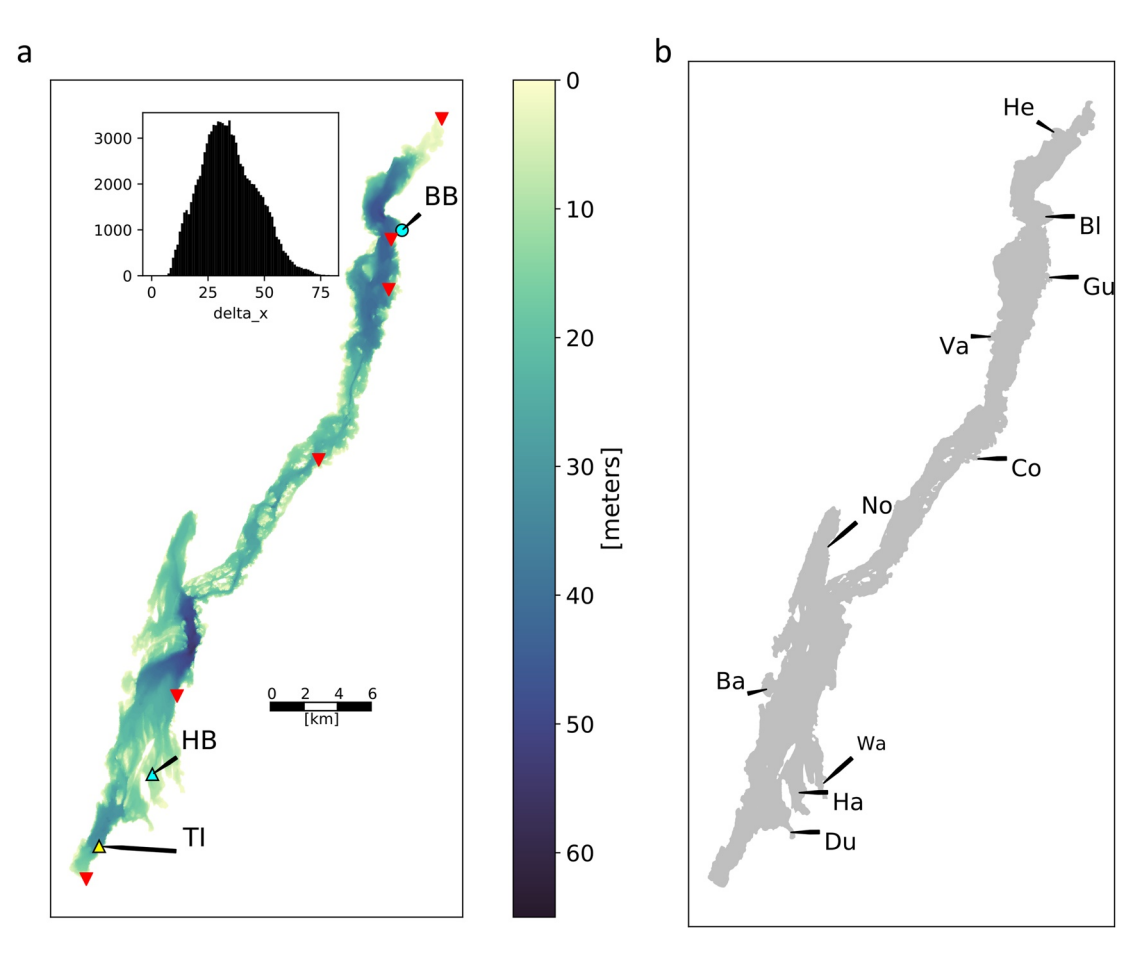


Figure 1. (a) Bathymetry of Lake George, New York, displayed with color scale. Red triangles represent the location of weather stations around the lake. The yellow triangle represents the locations of the vertical profilers in the south basin (Tea Island-indicated by TI) and the cyan triangle represents the location of the vertical profiler equipped with an Acoustic Doppler Current Profiler (ADCP) at Harris Bay (indicated by HB). The cyan circle represents the location of ADCP measurements in Blairs Bay (indicated by BB). The inset histogram depicts the distribution of horizontal resolution across the grid for the Stanford Unstructured Nonhydrostatic Terrain-Following Adaptive Navier-Stokes Simulator model. (b) Location map of the 10 bays that were used in the simulation of water age. Du, Dunham Bay; Ha, Harris Bay; Wa, Warner Bay; Ba, Basin Bay; No, Northwest Bay; Co, Cook Bay; Va, Van Buren Bay; Gu, Gull Bay; Bl, Blairs Bay; He, Heart Bay.

a frequency of 0.4 Hz, mounted on the platform of the vertical profiler. Profiling depth was started 1.25 m below the surface and was discretized into 0.25 m bins. In the post-processing step, we split the timeseries into 15-min long sections and took the time average of each section. At the beginning of the deployment, limited sunlight on the solar panels on the vertical profiler reduced the number of collected profiles. About 4-day worth of vertical profiles were missed due to that issue.

On 28 April 2022, we conducted an opportunistic transect using a downward-looking 1,200 kHz Workhorse Acoustic Doppler Current Profiler (ADCP; Teledyne RD Instruments) from a small boat in Blairs Bay (Figure 1a). Because the water is shallow at this deployment site (approximately 2.5 m), we set the ADCP to collect data in high resolution mode, which recorded measurements of current profiles with a vertical resolution of 5 cm, beginning 30 cm below the surface. After averaging the current profiles when the boat was anchored, we obtained water currents in Blairs Bay at two locations.

#### 2.3. Hydrodynamic Models

We simulated water currents and temperature within Lake George using the numerical model Stanford Unstructured Nonhydrostatic Terrain-Following Adaptive Navier-Stokes Simulator (SUNTANS) (Fringer et al., 2006). The model utilizes an unstructured grid in the horizontal plane, and *z*-levels in the vertical plane. The surface boundary conditions are estimated at each time step based on the simulated water temperature, currents, and meteorological inputs from the daily forecasts generated by the Weather Research and Forecasting (WRF)-based

AUGER ET AL. 3 of 17

weather model with a horizontal resolution of 1 km. A more detailed description of the weather model can be found in Auger et al. (2021).

We performed a simulation to characterize water age and hydrodynamics in high spatial resolution within bays. The fine grid portion has an average horizontal resolution of 50 m, and areas of increased resolution used within bays made use of an average grid cell size of 30 m. We selected a total of 10 bays, distributed around the lake with a wide range of surface areas. The largest (Northwest Bay), with an area of 5.06 km², the smallest (Cook Bay), with an area of 0.094 km² (see Figure 1b for a site map). We set the vertical discretization to be finer close to the surface of the lake ( $\Delta z \sim 0.73$  m) and coarser at the deepest areas of the lake ( $\Delta z \sim 1.3$  m) for a total of 57 layers. To ensure that topographical effects on water currents in smaller bays are taken into consideration in the simulation, we interpolated the water depth onto the grid from a high-resolution bathymetrical survey of Lake George.

We coupled WRF and SUNTANS in a one-way framework, where the results of weather simulation drove the hydrodynamics, but the hydrodynamic model outputs do not influence the weather model. WRF model outputs provide easting and northing components of the wind vector at 10 m above surface and variables required for the computation of heat fluxes (air temperature, air pressure, and relative humidity), including downward longwave and shortwave radiations. To estimate the appropriate heat loss from the lake, net heat fluxes are computed within the hydrodynamic model at each time step. Instead of using constant exchange coefficients for heat fluxes and wind stress, we computed the coefficients using the COARE3 algorithm (Fairall et al., 2003). We initialized the model with a lake at rest and a uniformly distributed water temperature at 4.0°C. We had the model simulate the lake hydrodynamics from 19 April 2022, midnight UTC until 17 June 2022, midnight UTC, for a total of 59 days. During this time, we assumed the lake was a closed system, with no lateral inflow or outflow, to estimate the upper range of water age in Lake George. We consider the first week of the simulation (19–26 April 2022) as the spinup period. The wall-clock time of the hydrodynamic simulation reached 7 days on a system with 88 cores. This period was chosen to capture springtime dynamics and the beginning of the stratification period in Lake George, when biological activity increases to summer levels.

We analyzed the distribution of sub-basin water age using the capability implemented within the SUNTANS model, as described by Rayson et al. (2016). The usage of water age allows us to generate snapshots of a proxy to residence time that can be linked to weather events. Water age involves the introduction of two additional numerical tracers ( $\alpha$  and C) in the numerical model. We briefly describe these two variables and how they are used in the simulation run. For a thorough explanation of these variables, the authors refer the readers to Deleersnijder et al. (2001), Delhez et al. (1999), and Rayson et al. (2016) for the implementation in SUNTANS.

Within a volume of fluid centered on the three-dimensional point  $\mathbf{x} = (x, y, z)$ , all the particles of an element in this volume do not necessarily have the same history, and consequently not the same age  $\tau$ . Therefore, there exists a concentration distribution function,  $c(t, \mathbf{x}, \tau)$ , from which we can compute the concentration of the element in this volume by  $C(t, \mathbf{x}) = \int_0^\infty c(t, \mathbf{x}, \tau).d\tau$ . Similarly, we can compute the age concentration  $\alpha(t, \mathbf{x}) = \int_0^\infty \tau.c(t, \mathbf{x}, \tau).d\tau$ , for each volume of fluid. The transport of  $\alpha(t, \mathbf{x})$  and  $C(t, \mathbf{x})$  are governed by the following governing equations:

$$\frac{\partial C}{\partial t} + \nabla \cdot (\boldsymbol{u}C) = \frac{\partial}{\partial z} \left( K_T \frac{\partial C}{\partial z} \right)$$

$$\frac{\partial \alpha}{\partial t} + \nabla \cdot (\boldsymbol{u}\alpha) = \frac{\partial}{\partial z} \left( K_T \frac{\partial \alpha}{\partial z} \right) + C$$

The advection and mixing of  $\alpha(t, \mathbf{x})$  and  $C(t, \mathbf{x})$  are performed alongside water temperature within SUNTANS by using existing scalar transport function. The mean age of each grid cell,  $a(t, \mathbf{x})$ , can be evaluated by  $a(t, \mathbf{x}) = \frac{\alpha(t, \mathbf{x})}{C(t, \mathbf{x})}$ .

The boundary conditions were set up to answer the question how long water from the main basin remains in the bay before being flushed out by the currents driven by the weather conditions. For every bay shown in Figure 1, we assigned the condition that water crossing the mouth of the bay have an age concentration  $\alpha = 0$  and a concentration C = 1 to allow the water entering the bays to age until it leaves the bays. The boundary conditions presented here resemble that of Rayson et al. (2016) for Galveston Bay, Texas, though our analysis differed in that we included multiple small embayments with no inflow from streams. Tracers  $\alpha$  and C are simulated in the main basin of the lake but are not analyzed here. The residence time of Lake George is estimated to be around 6.8 years (Shuster et al., 1994 in Swinton and Boylen (2014)), the simulation performed here is too short to obtain

AUGER ET AL. 4 of 17

relevant simulation outputs of water age for the entire lake, but will highlight the short-term variability of water age in the bays. Snapshots of water age distribution in Blairs Bay, displayed in Figure S1 in Supporting Information S1, show an overall similar spatial distribution in the simulation. They also illustrate differences that reflect the short-term changes.

#### 3. Results

## 3.1. Validation

We compared our simulation results against water temperature profiles obtained from the *TI* and *HB* profilers moored in the south basin of Lake George. We also compare the simulated water currents against ADCP data collected in Blairs Bay. We present the results of water temperature comparison in a Taylor Diagram (Figure 2a) alongside the heatmaps of water temperature collected with our vertical profilers. To visualize all the variables from the water temperature validation in a single Taylor Diagram, we normalized the coordinates by the standard deviation of the observation.

Our results show that simulated water temperature from *HB* is consistent with sensor observations over space and time. The correlation coefficients are greater than 0.95 and the normalized Root Mean Squared Differences of the anomalies are lower than 0.25. From the heatmap representation, the surface water in the simulation is warmer than what was observed. Simulated water temperatures at *TI* demonstrated a larger departure from sensor data than was found in *HB*, specifically for temperatures at depth greater than nine m. However, the correlation between observation and simulation remains above 0.6. The heatmap representation indicates that the simulated thermocline stands shallower in the water column than the observed thermocline, which explains the larger error shown in the Taylor Diagram for *TI* profiler. We notice that simulated deep water (deeper than 20 m) remains colder than observations, and similarly to *HB*, we notice that the surface water is warmer in the simulation.

#### 3.2. Water Current Validation With ADCPs

We compared ADCP measurements made in Blairs Bay with model outputs (Figure 2d). The shallowest measurements we have from the ADCP transects are from 0.3 m depth, representing surface currents at this site. The comparison shows that simulated surface currents were consistent with observation at that time, with consistent directions and an overestimation of 0.03 m/s at both locations. The simulation suggests water was flowing into the head of the bay at the north end, and outward at the south.

Figures 2e and 2f show timeseries of observed and simulated eastward currents and northward currents, respectively, at two depth levels (1.3 and 5.0 m depth) in Harris Bay. The numerical model simulated consistent water currents (amplitude and direction) to the observation data. In both the simulation and observation data, the eastward component of velocity remained within the range of [-0.05, 0.05] m/s. On various occasions the northward component of the velocity at the surface and mid-column exhibited amplitudes greater than 0.05 m/s. Because Harris Bay is mainly oriented along the north/south axis of the lake, a difference in amplitude in the velocity components is expected. Moreover, the head of Harris Bay is in the south end of the bay, northward currents recorded by the ADCP and simulated by the model indicate water leaving the bay.

#### 3.3. Water Current Activity Within the Bays

To illustrate the kinematic activity within some of the bays, we computed the bay-average water current magnitude, which is related to the kinetic energy per cubic meter of each bay, at each time step. Figure 3 shows the distribution of the volume-average water velocity magnitude in four bays (Northwest Bay, Harris Bay, Blairs Bay, and Basin Bay) and within the whole lake. As seen in Figure 3a, the distribution of lake-average magnitude of velocity vectors displays a somewhat similar shape to those found in Harris Bay. The median and 90%-percentile for the lake-average currents magnitude approximate to 0.019 and 0.035 m/s, respectively, and for Harris Bay they are 0.016 and 0.036 m/s, respectively. The similar distributions in the whole lake average and those from Harris Bay indicate similarities in volume average of water current magnitude, which is reflected in the similarities in median and 90%-percentile values. However, we observe differences in distributions between the whole lake and within Basin Bay (Figure 3b). Bay-averaged currents are substantially smaller than the whole lake (median: 0.013 m/s, 90% percentile: 0.026 m/s for Basin Bay).

AUGER ET AL. 5 of 17

1944/973, 2024. 2, Downloaded from https://agupubs.onlinelibrary.wiley.com/doi/10.1029/2022WR034168 by Rensselser Polytechnic Institute, Wiley Online Library on [04/04/2024]. See the Terms and Conditions (https://onlinelibrary.wiley.

conditions) on Wiley Online Library for rules of use; OA articles

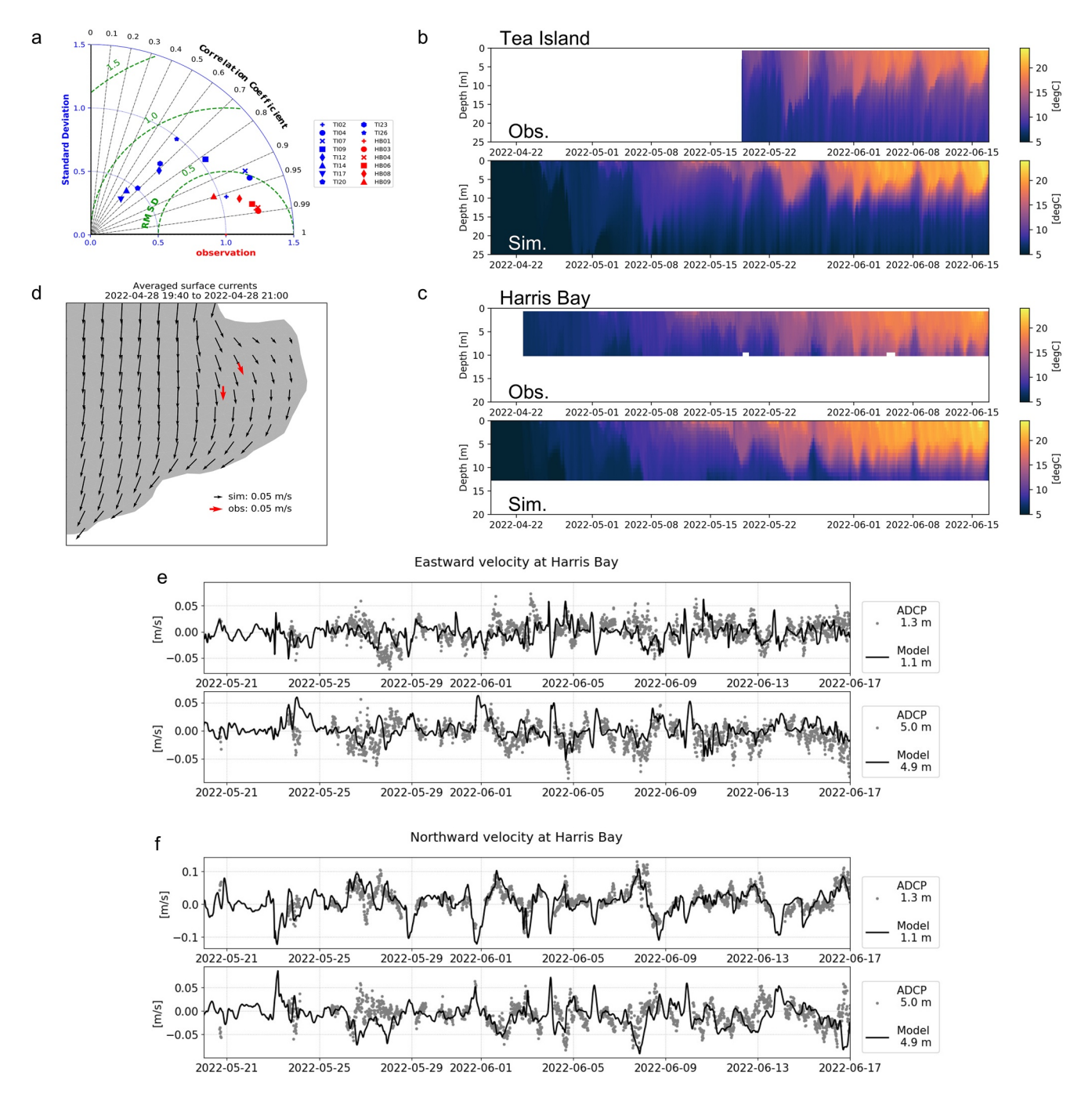


Figure 2. (a) Taylor diagram for the time when observed water temperature was available. Blue symbols represent temperature at Tea Island at several depths (TI## where ## stands for the depth in meter). Red symbols represent the temperature at Harris Bay. (b) Observed water temperature (top) and simulated water temperature (bottom) at Tea Island. (c) Observed water temperature (top) and simulated water temperature (bottom) at Harris Bay. (d) Observed surface currents from the Acoustic Doppler Current Profiler (ADCP) (in red) overlaid on the simulated surface currents (in black). (e) Observed eastward velocity (gray dots) against simulated eastward velocity (black line) at around 1.1 m depth (top) and 5 m depth (bottom). (f) Observed northward velocity (gray dots) against simulated northward velocity (black line) at around 5 m depth (bottom).

The distribution of velocities in Northwest Bay (Figure 3c), one of the large bays of Lake George (surface area of 5 km²), shows consistency with the distribution for the lake-average value. Specifically, similar median and 90% percentile velocity values (for Northwest Bay, median: 0.016 m/s, 90% percentile: 0.035 m/s) to the lake averaged case. Similarly, the distribution from Blairs Bay (located in the northern basin of Lake George, with approximately the same surface area as Basin Bay) indicates substantially lower velocity magnitude (median: 0.009 m/s, 90% percentile: 0.018 m/s) in the bay compared to those from the whole lake.

AUGER ET AL. 6 of 17

1944/973, 2024, 2, Downloaded from https://agupubs.onlinelibrary.wiley.com/doi/10.1029/2022WR034168 by Rensselaer Polytechnic Institute, Wiley Online Library on [04/04/2024]. See the Terms

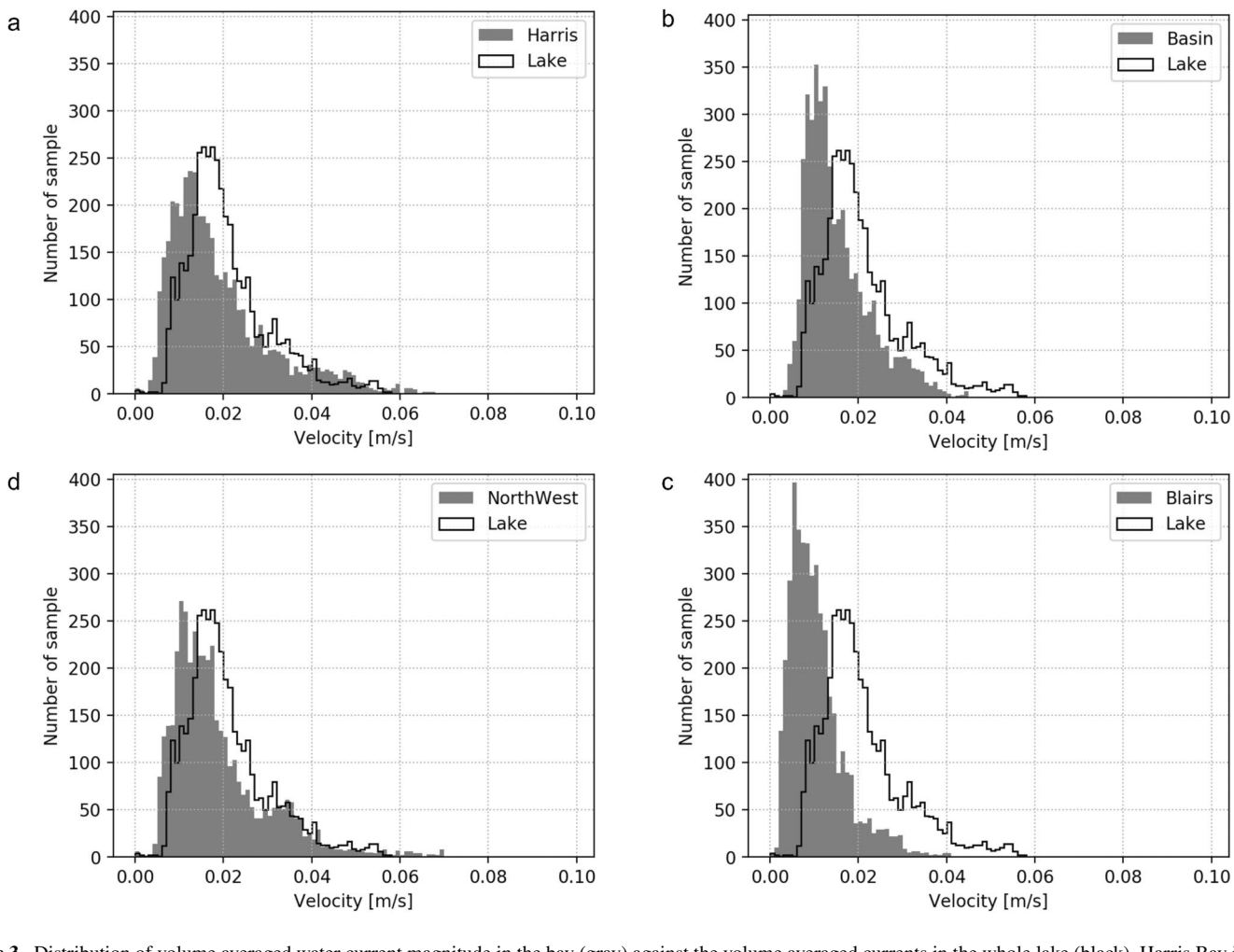


Figure 3. Distribution of volume averaged water current magnitude in the bay (gray) against the volume averaged currents in the whole lake (black). Harris Bay is represented in (a), Basin Bay in (b), Blairs Bay in (c), and Northwest Bay in (d).

As expected, the averaged velocity magnitude decreased as bay size decreased. The averaged velocities of the larger bays were similar to the whole lake mean whereas smaller bays had velocity magnitudes of approximately half of the whole lake. Even though the median velocities appear low, a magnitude of 0.01 m/s translates to a dwell time in a 1 m<sup>3</sup> volume of water of less than 2 min. However, the impact of the velocity at the scale of the bays will differ from one bay to the next.

### 3.4. Water Age Distribution During Wind Events

The distribution of volume averaged water currents magnitude shows that the bays of Lake George demonstrate a lower water current magnitude than the main basin of the lake. However, the difference is less than an order of magnitude. We investigated the influence of the water currents onto timescales in the bays by using the simulated water age scalar, and how it changes over time with weather conditions. For conciseness, we limit the analysis for this section to the following bays: Harris Bay, Blairs Bay, Basin Bay, and Northwest Bay. Figure 4 describes the distribution of water age within the bays and how it changes over time, plotted alongside the magnitude and the direction of the wind. The trend of the bay-averaged water age timeseries highlights the stability of Harris and Basin bays, whereas we see an increasing trend for Northwest and Blairs bays. However, the average water age for Blairs Bay (Figure 4a), Harris Bay (Figure 4b) and Basin Bay (Figure 4d) remained below 6 days throughout the simulation run. In the simulation, the bay-averaged water age in Northwest Bay increased up to 10 days after 60 days of simulation (Figure 4c). Moreover, a sharp decrease in the bay-averaged water age occurred during a wind event, where, in some instances the bay-averaged water age can lose 30% of its value within 1 day. This

AUGER ET AL. 7 of 17

19447973, 2024, 2, Downloaded from https://agupubs.onlinelibrary.wiley.com/doi/10.1029/2022WR034168 by Rensselaer Polytechnic Institute, Wiley Online Library on [04/04/2024]. See

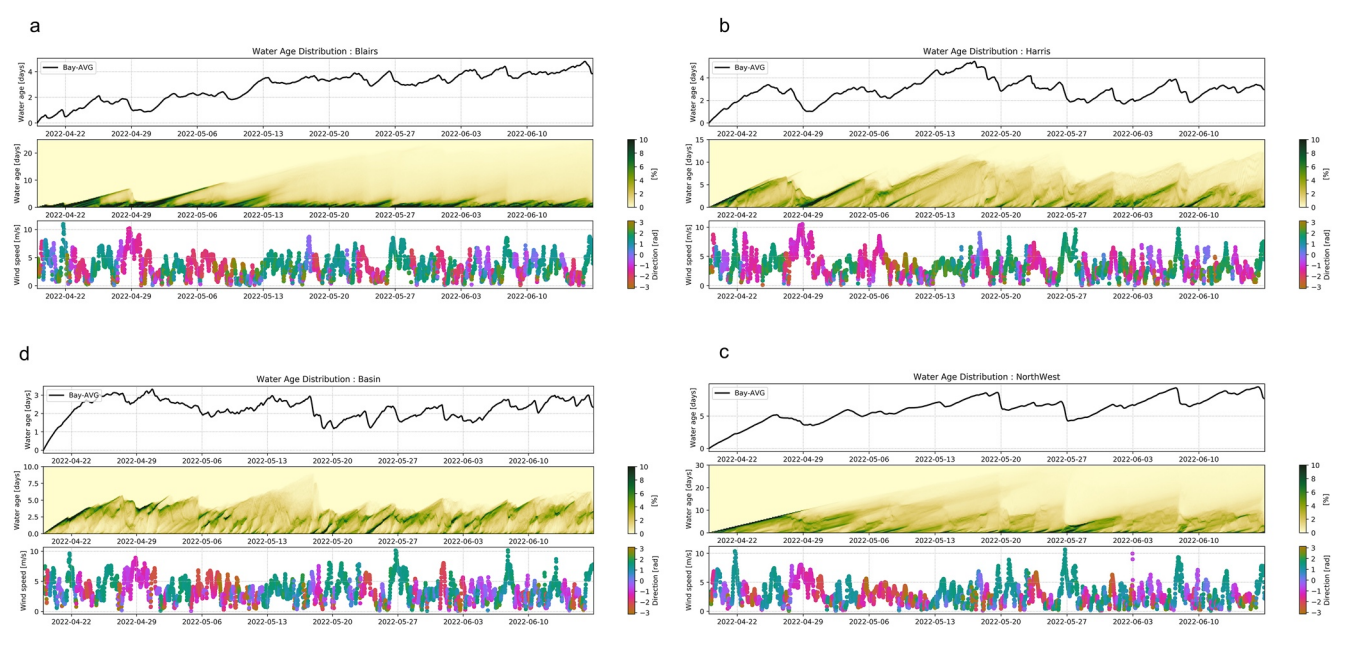


Figure 4. (a) Blairs Bay, (b) Harris Bay, (c) Northwest Bay, and (d) Basin Bay. For each bay: Top panel—Evolution over time of bay average water age. Middle panel—Change over time of the distribution of water age in the bay, the ordinate represents the bins of water age, the color represents the proportion of each bin. Bottom panel—Time series of wind speed magnitude with the color representing the angle at which the wind blows to 0 radians is toward east,  $\pi/2$  radians is toward north, and  $-\pi/2$  radians is toward south.

suggests that at the daily timescale, a substantial portion of the water in the bay can be transported into the main body of the lake.

Two typical wind patterns exist above Lake George: winds blowing toward the southeast and winds blowing to the north/northeast. During the simulation run, temporal changes in distribution of water age in the bays (Figure 4) appear to correlate to wind speed in the vicinity of the bays. For example, around 7 May, a sustained wind blew toward the southeast with velocities above 5 m/s for a day (Figure 4). We found the distribution of water age narrowed after this wind event for Basin Bay and Harris Bay. In Basin Bay, the distribution range was [0, 5.5] before the wind and [0, 3] after. The disappearance of older water in the distribution indicates an inflow of newer water from outside the bay mixing with the water within the bay. On 27 May, a strong wind blowing toward the north/northwest was present, with velocities above 7 m/s. Following this event, we found a narrowing of the water age distribution for all the bays. Because the bays are located in different parts of the lake and on either shore of the lake, the impact of the wind on water age will differ. This is illustrated by a narrowing of the distribution range in Harris Bay and Basin Bay during the southeastward wind but not in the other bays. For example, the distribution range was [0,4] for Blairs Bay before the wind event and [0,2] afterward.

In the next two subsections of the paper, we look at the spatial distribution of daily average water age during two wind events and after them. We focus on four bays: Northwest Bay, Harris Bay, Blairs Bay and Basin Bay. Harris Bay and Basin Bay are located on the eastern shore and Northwest Bay and Blairs Bay on the western shore.

## 3.4.1. Wind Toward Southeast

On 7 May, a wind blowing toward the southeast blew for 18 hr, with magnitude above 5 m/s. The wind event was associated with a narrowing of the water age distribution and a decrease of the volume averaged water age. Despite both bays being on the eastern shore, Harris Bay and Blairs Bay exhibited different patterns in daily averaged water age during the 7 May wind event (Figures 5a and 5c). A layer of water that had remained inside Blairs Bay for more than 4 days can be seen in the transect of Blairs Bay, whereas the water age transect in Harris Bay displayed an almost homogeneous distribution in the vertical and a gradual increase in water age from the mouth to the head of the bay. At the end of the transects, close to the shore, the transects highlight additional differences between the two bays: In Blairs Bay, the water age remains less than 3 days, whereas in Harris Bay the water age is greater than 5 days.

On 9 May, after the southeast wind event, the daily averaged water age along the transect exhibits discrepancies between the two bays. In Blairs Bay (Figure 5b), the water age distribution is similar to the time period during

AUGER ET AL. 8 of 17

1944/973, 2024, 2, Downloaded from https://agupubs.onlinelibrary.wiley.com/doi/10.1029/2022WR034168 by Rensselaer Polytechnic Institute, Wiley Online Library on [04/04/2024]. See the Term

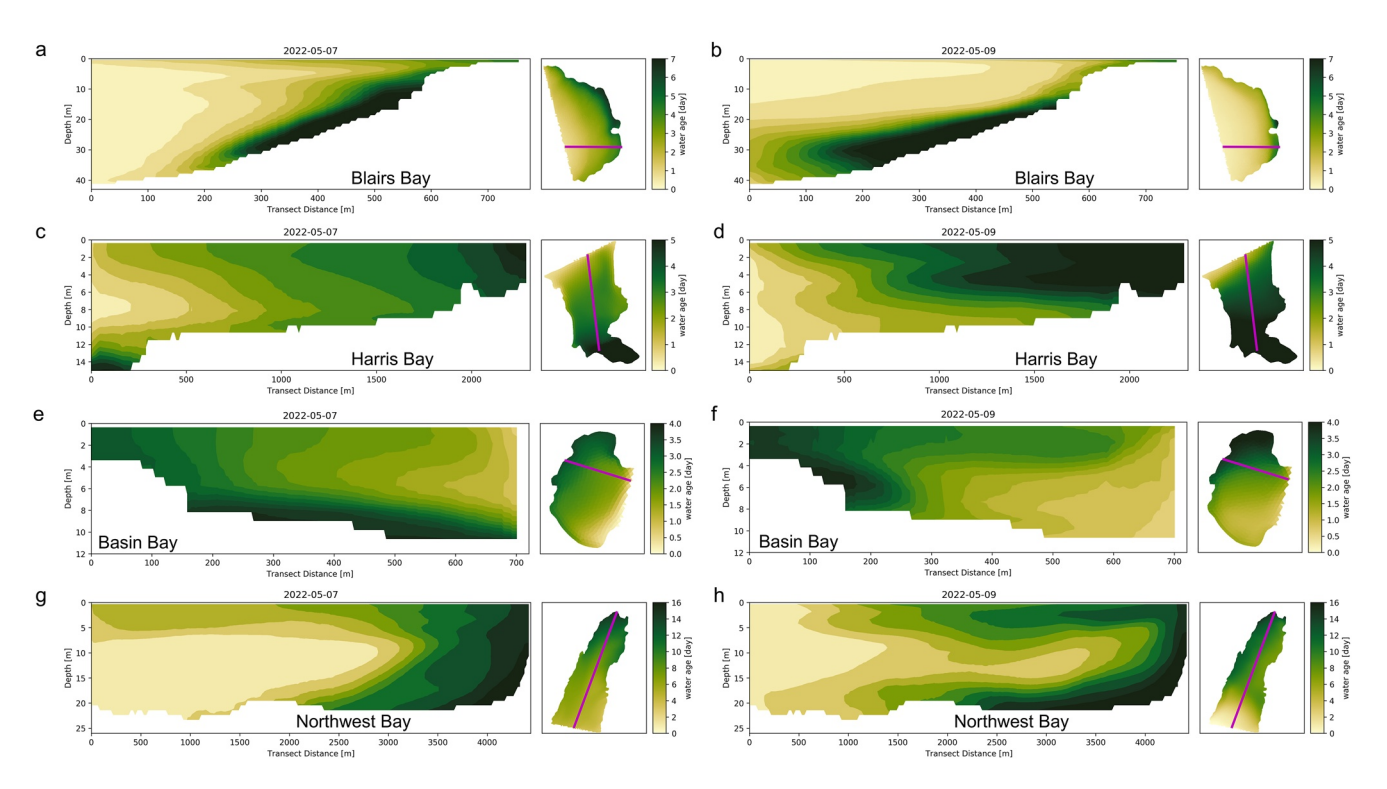


**Figure 5.** Daily average of water age along a transect in during a wind blowing southeast (7 May 2022) and after the wind event (9 May 2022) for each bay. (a, b) For Blairs Bay, (c, d) for Harris Bay, (e, f) for Basin Bay, (g, h) for Northwest Bay. Each transect is accompanied with the daily averaged water age at the surface, and the location of the transect with the magenta line.

the wind event. With older water (water age greater than 7 days) along the bottom of the bay, and water less than 2 days old found close to the surface. In Harris Bay (Figure 5d), the spatial distribution of water age suggests an intrusion of water from the main basin along the bottom of the bay during the wind event. Additionally, a layer of water older than 4 days was found closer to the mouth of the bay.

On the western side of the lake, we examined Northwest and Basin Bays. During the wind event on 7 May, the vertical distribution of daily-averaged water age in Basin Bay (Figure 5e) contained water with an age greater than 4 days above the bottom of the bay and younger water closer to the surface. In Northwest Bay (Figure 5g), the water at the head of the bay has remained in the bay for more than 7 days at depth as well as at the surface. However, the mid-column water has remained in the bay for less than 2 days. A mid-column intrusion of water from the main basin is suggested by a substantial decrease in water age deeper than 10 m. After the wind event, older water (water age greater than 2 days) remained close to the surface and newer water remains deep in the water column for Basin Bay (Figure 5f). Whereas the age distribution in Northwest Bay after the wind event shows a layer of water with an age less than 4 days in the middle of the water column, and older water (water age greater than 10 days) at the top and bottom of the water column (Figure 5h).

## 3.4.2. Wind Toward the North

On 27 May, a wind blowing toward the north was present for 12 hr, with a magnitude above 7 m/s, which was associated with a narrowing of the water age distribution and a decrease in the volume averaged water age in all the displayed bays. The transect of daily average water age for Blairs Bay (Figure 6a) shows a similar distribution on 7 May when the water above the bottom remained in the bay for more than 7 days. On the same day, the distribution of water age in Harris Bay (Figure 6c) suggests that water older than 4 days stays close to the surface and in shallow areas of the bay, with newer water found deeper in the water column and along the bottom.

On 30 May, after the northerly wind event, the distribution of water age in Blairs Bay (Figure 6b) is similar to the time period during the wind event, which can be attributed to the fact that stratification was present (See Figure 2), limiting the direct impact of wind forcing deep in the water column. In Harris Bay (Figure 6d), a 2 m-thick layer of older water (water age greater than 4 days) stands above the bottom of the bay, whereas water age in the rest of the bay remains less than 3 days (younger water found close to the mouth of the bay).

AUGER ET AL. 9 of 17

19447973, 2024, 2, Downloaded from https://agupubs.onlinelibrary.wiley.com/doi/10.1029/2022WR034168 by Rensselaer Polytechnic Institute, Wiley Online Library on [04/04/2024]. See the Terms

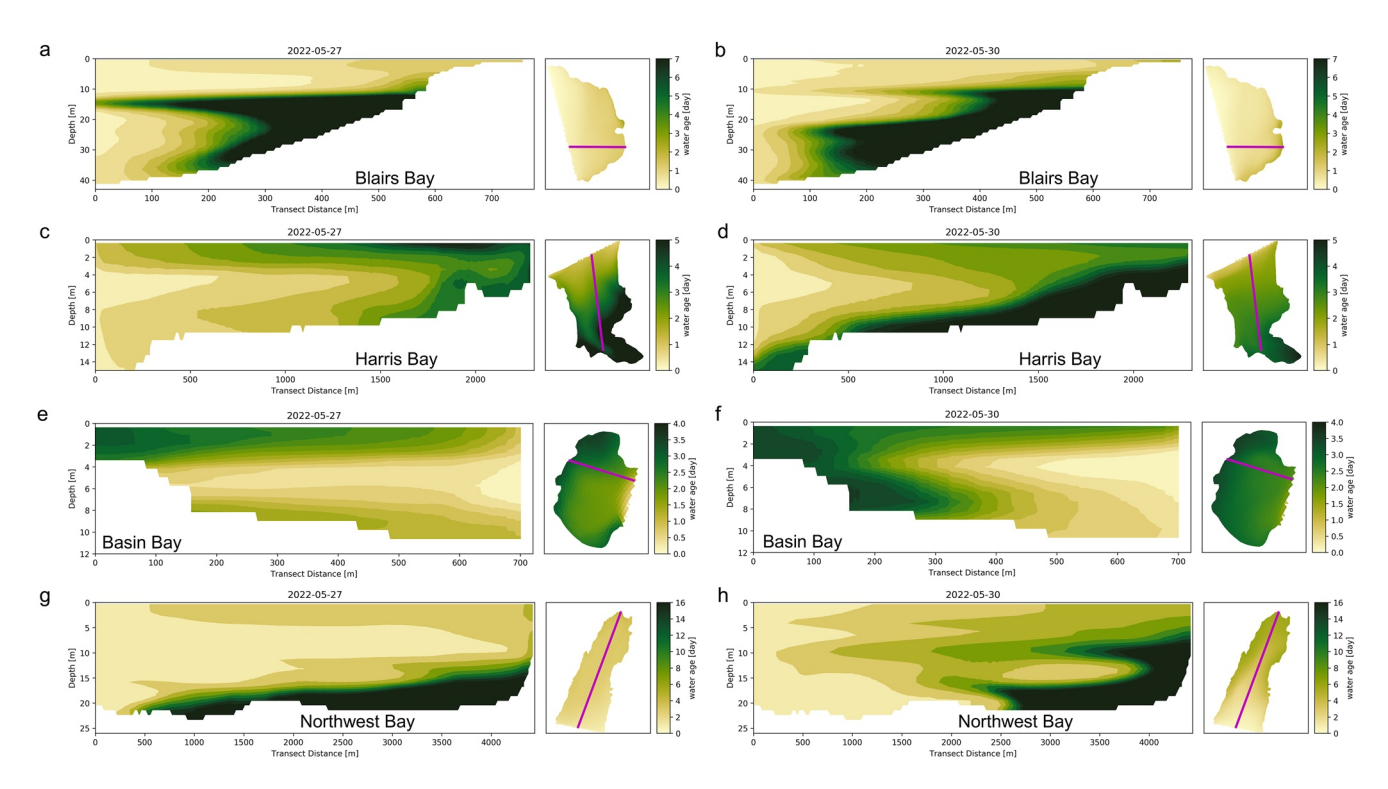
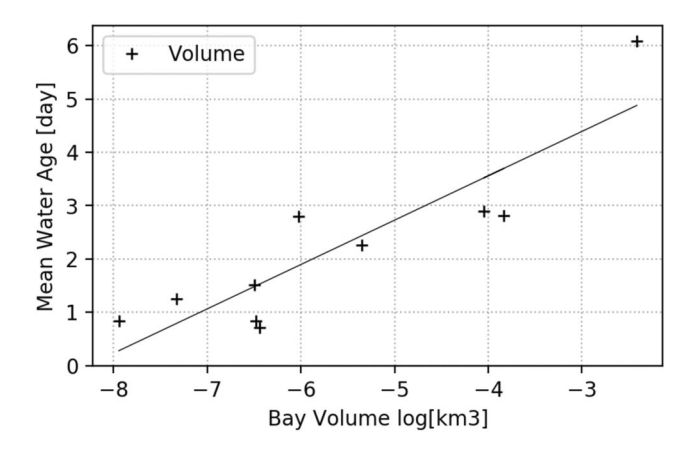


Figure 6. Daily average of water age along a transect in during a wind blowing northward (27 May 2022) and after the wind event (30 May 2022) for each bay. (a, b) For Blairs Bay, (c, d) for Harris Bay, (e, f) for Basin Bay, (g, h) for Northwest Bay. Each transect is accompanied with the daily averaged water age at the surface, and the location of the transect with the magenta line.

On 27 May, during the northerly wind event, the transect of simulated water age at Basin Bay (Figure 6e) suggests the presence of water close to the surface has remained in the bay for more than 2 days. In the rest of the bay, the water age distribution exhibits lower values (water age values less than 1 day), with a small increase of water age above the bottom of the bay with (water age of 1.5 days). In Northwest Bay (Figure 6g), a 5 m-thick layer of water with an age greater than 16 days remains above the bottom, whereas the water above that layer shows an age less than 4 days. After the wind event, on 30 May, the distribution of water age averaged over 24 hr demonstrates that surface and bottom water in Basin Bay (Figure 6f) is relatively older (3 days) than



**Figure 7.** Scatter plot of the mean water age against the volume of the bays (black crosses), in natural log scale. The thin black line represents the linear regression of the natural logarithm of bay area and mean water age (see text for the expression).

mid-column (1 day). In Northwest Bay (Figure 6h), the thick layer of older water (age greater than 16 days) close to the bottom was affected by the wind event, although this layer appears to concentrate closer to the head of the bay. Close to the surface, the water is relatively young with a water age no greater than 4 days.

#### 3.4.3. Spatiotemporal Averaged Water Age

Temporal changes in volume averaged water age (Figure 4) highlight the difference in scales between the different bays. The volume average in Basin Bay remained less than 3 days, whereas in Northwest Bay most of the volume averaged values are above 5 days.

The average water age, in time and in space, exhibits a relationship with the surface area of the bays, with large bays being associated with a greater water age (Figure 7). We estimate the average water age in the largest bay, Northwest Bay, to be 6 days, whereas the smallest bay, Cook Bay, to be 0.8 days. The averaged water age was correlated with the natural log of the bays' volume. Using linear regression, we estimate the relationship between the two variables to be  $WA = 0.83 \times log(BV) + 6.9$ , where WA is the water age,

AUGER ET AL. 10 of 17

 Table 1

 The First Row Displays the Mean Ratio r, Defined as KE\_barotropic/KE\_baroclinic, Across the Mouth of Each Bay

	Blairs	Basin	Harris	Northwest	Warner	Vanburen	Cook	Heart	Gull	Dunham
Mean	0.15	0.58	0.21	0.2	0.2	0.13	0.23	0.4	0.16	0.18
Median	0.09	0.21	0.08	0.07	0.1	0.07	0.1	0.22	0.09	0.09

Note. The second row displays the median value of the ratio for each bay's entrance.

in days, and BV is the volume of the bay in  $km^3$ . The regression has a standard error of 0.15 days and a p-value lower than 0.01.

## 3.5. Physical Processes Involved in the Changes in Water Age in the Bays

In this section, we investigate the physical processes involved in the changes of water age within the bays. In thermally stratified water, we differentiate between currents generated by a spatial gradient of water surface elevation (barotropic) and the currents generated by a spatial gradient of water density (baroclinic). We computed the barotropic currents, Ubt, at each grid cell as the vertically integrated water velocity and divided by the depth at the grid cell:

$$Ubt = \frac{1}{D} \sum_{k=0}^{N} U_k \times \Delta z_k$$

where D represents the total water depth at the grid cell,  $U_k$  is velocity vector at layer k simulated by the hydrodynamic model. N represents the number of active layers in the water column.  $\Delta z_k$  represents the thickness of the layer k, where  $\Delta z_{k0}$  includes the free surface elevation  $\eta$ . We compute the baroclinic velocity, Ubc, by subtracting the barotropic velocity to the simulated velocity:

$$Ubc(z) = U(z) - Ubt$$

To assess which component dominates the hydrodynamics at the mouth of the bays, we look at a the kinetic energy, estimated from the integration of the squared velocity normal to the mouth of the bays.

The comparison of the kinetic energy at the mouth of each bay shows that baroclinic dynamics are dominant in all the bays (Table 1). The mean ratio of barotropic energy over baroclinic energy indicates it hovers around 20% in all the bays, except for Basin Bay and Heart Bay, where the ratio reaches 60% and 40%, respectively. The median of the ratio is about half of the mean value, suggesting there are times where baroclinic kinetic energy was substantially greater than the barotropic energy. Time series of both components of kinetic energy (Figure S2 in Supporting Information S1) show that in a couple of occasions, barotropic kinetic energy becomes dominant, for example, in the end of April 2022 in Harris Bay, when the lake was weakly thermally stratified. However, during the strongly stratified period, baroclinic kinetic energy is dominant, by a factor of 5 (Figure S2 in Supporting Information S1). We can conclude in this section that baroclinic currents are likely to be responsible in the changes in bay-average water age, rather than barotropic currents.

Baroclinic physical processes represent the hydrodynamics originating from spatial gradients in water density, especially changes in depth of thermocline's depth. Because changes in thermocline's depth will be illustrated in the values of potential energy anomaly in the system, we estimated the potential energy anomaly in the system as follows:

$$PE_{anom}(t) = PE(t) - PE_0$$
 with

$$PE(t) = \sum_{i} A_{i} \sum_{k=0}^{Ni} g \times \rho_{k,i} \times z_{k,i} \times \Delta z_{k,i}$$

The variable  $PE_0$  represents the potential energy at the initial time step. The variable  $\rho_{k,i}$  is the water density in the vertical layer k of water column i. The constant g represents the gravitational constant,  $z_{k,i}$  the depth of the layer k at mid-level, and  $\Delta z_{k,i}$  the thickness of the layer. The thickness of the top-layer,  $\Delta z_{0,i}$ , includes the impact of the free-surface elevation. Ni is the total number of active vertical layers in the water column i and  $A_i$  represents the area of the grid cell i.

AUGER ET AL. 11 of 17

1944/7973, 2024, 2, Downloaded from https://agupubs.onlinelibrary.wiley.com/doi/10.1029/2022WR034168 by Rensselaer Polyaechnic Institute, Wiley Online Library on [04/04/2024]. See the Terms and Conditions (https://onlinelibrary.wiley.com/erms

conditions) on Wiley Online Library for rule

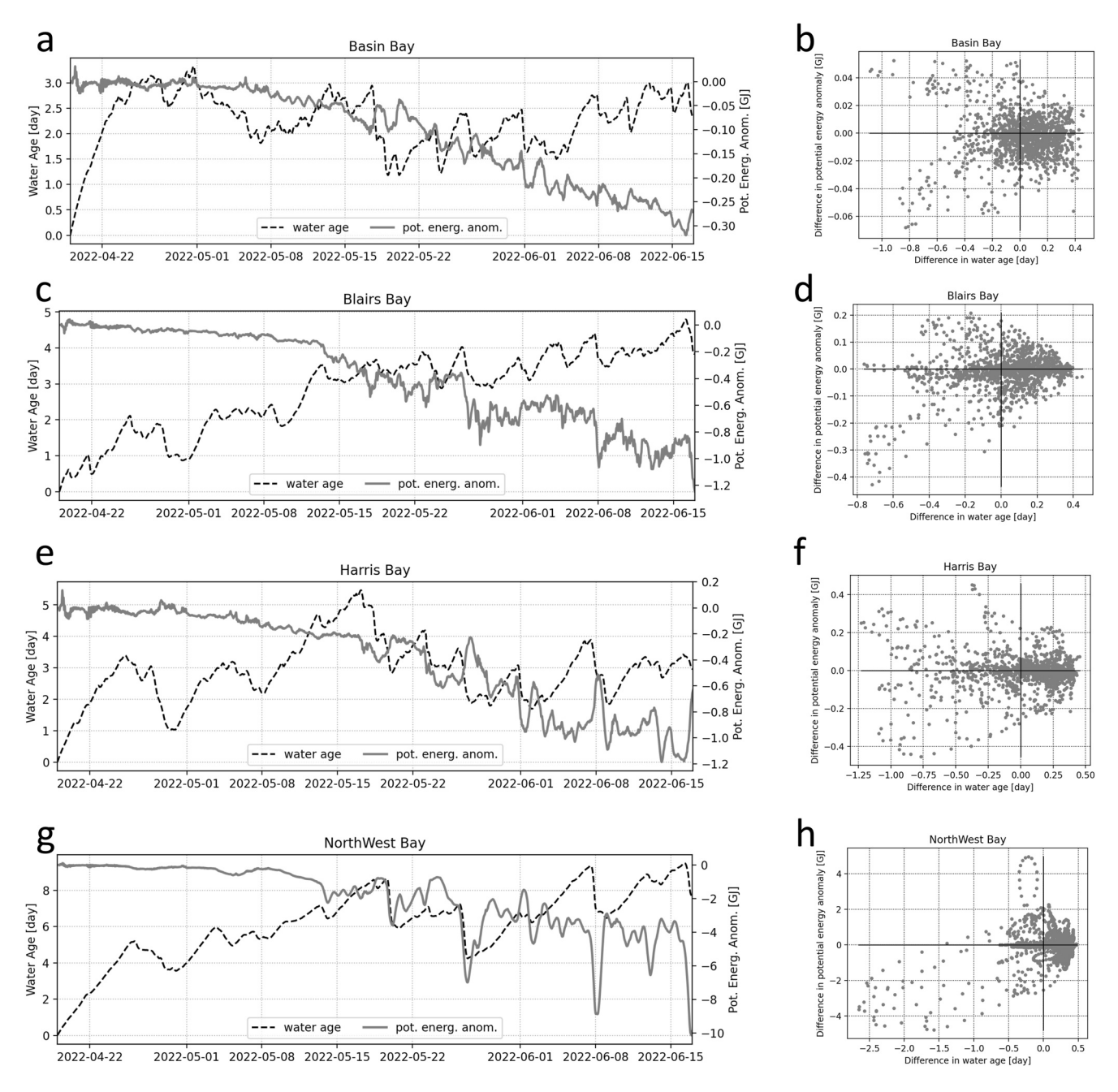


**Figure 8.** On the right pane, (a, c, e, g) show time series of potential energy anomaly (gray line) and bay average water age (black dashed line) for Basin Bay, Blairs Bay, Harris Bay and Northwest Bay, respectively. Panes (b, d, f, h) display the scatter plot of the difference in water age in 12 hr window (on the ordinate) and the difference in potential energy anomaly in a 12 hr window on the abscissa.

The long-term trend in the potential energy illustrates the warming and stratification of the water column for all the bays (Figure 8). As water temperature increases, water density becomes increasingly lower than the water density reference,  $\rho_0$ , hence potential energy anomaly being negative. In addition to the long-term trend, short term variations of potential energy anomaly take place. For example, in 27 May 2022, in Harris Bay, an increase of 0.4  $10^9$  J indicates a thicker layer with greater density, which is an indication the thermocline becomes shallower, defined as an upwelling. The upwelling in Harris Bay is visible in the heatmap of water temperature where the depth of the thermocline goes from 10 to 5 m deep. Substantial decrease in bay-averaged water age often correlates with substantial changes in potential energy anomaly. In Harris Bay, the bay-average water age decreases from 4.2 to 3 days on 22 May, and at the same time the potential energy anomaly decreases by 0.3  $10^9$  J. On 27 May, a

AUGER ET AL. 12 of 17

substantial decrease in water age (from 3.5 to 2 days) is correlated with a substantial increase of potential energy anomaly (+0.4 10<sup>9</sup> J). In Harris Bay, a decrease of water age was correlated to both downwelling and upwelling events (Figure 8), when the wind blew southward and northward, respectively (Figure S3 in Supporting Information S1). In Northwest Bay, Figure 8 shows substantial decreases in water age were correlated with a sharp decrease in potential energy anomaly. These decreases of potential energy anomaly occurred when a strong wind from the south-west blow into the bay (Figure S3 in Supporting Information S1).

To illustrate the correlation between substantial decrease in water age and changes in potential energy anomaly, we compute the 12 hr difference in these variables, 6 hr after minus 6 hr prior, and show the variables in a scatter plot (Figures 8b, 8d, 8f, and 8h). The correlation between negative temporal gradient in water age and negative gradients of potential energy anomaly suggests that in Northwest Bay, decrease of water age originates from a downwelling events in the bay. For Harris Bay, Blairs Bay and Basin Bay, negative temporal gradients of water age are associated with either positive or negative gradients of potential energy anomaly. Because baroclinic currents are characterized by vertical layers with opposite velocity direction, it is consistent that either a downwelling or an upwelling participates in the decrease of water age in the bay. In both cases, there is water flowing from the main basin into the bay, be it above or below the thermocline. Additional scatter plots using a time range of 14 and 18 hr, instead of 12 hr, to compute the temporal differences show the same pattern, where negative differences were associated with positive and negative differences of potential energy anomaly for Harris Bay, Blairs Bay and Basin Bay (Figure S4 in Supporting Information S1). Furthermore, changing the time range for the differences did not modify the conclusion on the correlation between downwelling events and decrease of water age in Northwest Bay.

#### 4. Discussion

The numerical results presented here indicate the simulated water age average in bays of Lake George remained on the scale of days (up to 6 days in Northwest Bay). Taking water age as a surrogate to residence time, our results show that residence times in the bays are very short compared with the residence time of the whole lake, which is estimated at 6.8 years. However, given that many physical, chemical, and biological processes can manifest themselves at temporal scales below this duration, these residence calculations indicate that spatial movement of water within large lakes may be a primary driver of heterogeneity observed through time at any given location. The mean water age values we simulated for the bays of Lake George fall in the same order of magnitude as the residence time (3.5 days) that was simulated in the shelf area of the main basin of Cayuga Lake, NY, by Gelda et al. (2015) and by Rueda et al. (2008) who found the transfer of tracers from a bay of Clear Lake, CA, to the main basin required 7 days. Although, water age and residence time are different time scales, Rayson et al. (2016) showed similarities between the two time scales in their study of Galveston Bay, Texas, and past studies have assumed water age to be similar to residence time (Duffy et al., 2018). Therefore, we interpret the temporal mean water age as an estimation of the average residence time in our results.

The increase of residence time with the volume of a lake (Figure S5 in Supporting Information S1) follows an exponential curve, we expected the mean water age to similarly increase with the volume of bays. However, we found the averaged water age increases with the volume of the bay, but not as rapidly as expected. This difference may originate from the fact that the average water age is estimated based on a 60-day long simulation, and the averaged water age for Northwest Bay, the largest bay of our study, trended upward even at the end of the simulation. We suggest that stratification and the elongated topography of the bay made deep water at the head of the bay isolated. If the simulation had continued further, we expect the average water age to increase according to this trend. Unfortunately, the cost of running the hydrodynamic simulation for a whole year would be prohibitive, since it would take approximately 1.5 months to perform the simulation.

The distribution over time of water age (Figure 4) in the bays indicates substantial changes in the distribution linked to wind events. As noted by Liu et al. (2020), the effect of wind speed as a driver will depend on wind direction and the geometry of the bays. When winds are aligned with the longest direction of bays then residence times will be more sensitive to variations in wind speed. Indeed, the distribution of water age in Northwest Bay, which is aligned north-south, becomes narrower during intense northerly winds. For example, on 20 May, the wind event led to a drop of mean water age in the bay (~30% of the original bay-averaged water age). Wind blowing toward the southeast, a predominant wind over Lake George, does not have a substantial impact on the water age distribution in Northwest Bay, especially after the development of stratification. The distribution of water age in the other three bays (i.e., Harris Bay, Blairs Bay, and Basin Bay) appears to be impacted by wind speed, regardless of the direction, although the wind blowing toward the southeast shows less impact compared

AUGER ET AL. 13 of 17

to the northward wind. For example, the volume-averaged water age within Harris Bay shows a drop of one day during southeasterly wind (See 6 May or 23 May in Figure 4) whereas a drop of 2 days is noticeable in the time series during northerly winds (27 May and 7 June).

In our results, we show that changes in the bay-average water age are mainly governed by baroclinic physical processes. In most of the studied bays, the decrease in water age was correlated with either a downwelling or an upwelling. However, in the case of Northwest Bay, the largest bay of Lake George, the decrease of water age was linked to downwelling events only. Moreover, the intensity of the down- or up-welling event mattered because substantial change in water age occurred when a change in thermocline depth is substantial as well. Interpretation of our results in Lake George's bays coincide with Rueda and Cowen (2005)'s conclusion in Little Sodus Bay in Lake Ontario. However, because they estimate the role of upwelling events based on a criterion using surface density only, they focus on complete upwelling, where metalimnetic or hypolimnetic water reaches the surface. Because they would not capture incomplete upwellings, the role of upwelling in their bay may be underestimated. In our work, we use the potential energy anomaly of the bay, we therefore capture the incomplete upwellings, and smaller decrease in water age in the bays.

The spatial distribution of water age can change drastically depending on the wind event and the bay in question. In some situations, the water age distribution after the wind event was reversed from the distribution during the wind event. In our modeling results, we observed older water close to the surface in Harris Bay during a northward wind (Figure 6c) whereas we observed the older water above the bottom after the wind event (Figure 6d). A similar interpretation can be made for Basin Bay when the wind blew toward the southeast. We found the older water above the bottom and close to the mouth of the bay during the wind event (Figure 5e), and after the wind event it was located close to the head of the bay (Figure 5f). These snapshots illustrate the drastic influence of meteorological forcing onto the spatial distribution of water age in Basin Bay. In addition to direct impact from the wind (Doda et al., 2022), looked at the effect of a thermal siphon on the flushing time in a littoral zone of Rotsee Lake, Switzerland. They estimated the timescale to be 10 hr. Thermal siphons are potentially ubiquitous in lakes as they result from differential heating due to sloping boundaries in lakes.

Among the four bays presented here (Figures 5 and 6), Blairs Bay is the only bay that was repeatedly found to have older water in the deeper parts of the water column, and relatively newer water close to the surface. Despite having relatively young water close to the surface, the bay-averaged water age trends upward throughout the simulation (Figure 4). The widening of the distribution range of water age alludes to a portion of the bay that sees an aging of water. The temporal average transect indicates that on a 60-day time scale (Figure 9), the water parcel forming a 5 m thick layer above the bottom has remained in the bay for more than a week. This layer begins once it is below the surface mixed layer, which is about 9 m thick (See Figure 2).

The averaged transect of water age in Van Buren Bay shares similarities in distribution with Blairs Bay (Figure S6 in Supporting Information S1). The transect of water age in Van Buren Bay, located on the western side of Lake George, exhibits a local maximum, with water age greater than 1.75 days below a depth of 12 m. Close to the head of the bay, the water has remained in the bay for less than 1.5 days. This is a similar distribution as seen in Blairs Bay, although the magnitudes are less in Van Buren Bay, most likely due to the differences in volume. Northwest Bay shares similarities with Blairs Bay, with both containing water older than 2 weeks in the bottom layer at the head of the bay. However, even though the water close to the surface is more recent than at the bottom, the water age is greater compared to Blairs bay (9 days in Northwest Bay compared 2.5 days in Blairs bay).

## 5. Conclusion

With a validated hydrodynamic simulation of Lake George, we investigated the mean water age and its distribution in 10 bays. Our numerical results from Lake George show that 9 out of the 10 studied bays have a mean water age (a surrogate for residence time) smaller than 3 days, and a further three bays had water ages less than 1 day. These relatively low ages indicate frequent exchange between bays and the main body of the lake. However, many physical, chemical, and biological processes can manifest themselves in a single day, and therefore these residence times may introduce temporal heterogeneity in water quality conditions when measured at a single location. Because our numerical setup implies a no-flow lateral boundary condition, these results are the upper range of water age and may be conservative estimates of water mass exchange around the lake. However, the bay-average water age shows that it can sharply decrease within one day due to a strong wind event. These decreases of water age in the bays were associated with substantial changes in thermocline depth, either upwelling or downwelling.

AUGER ET AL. 14 of 17

1944/793, 2024, 2, Downloaded from https://gupubs.onlinelibrary.wiely.com/doi/10.1029/2022WR034168 by Renseater Polytechnic Institute, Wiley Online Library on [04/04/2024]. See the Terms and Conditions (https://onlinelibrary.wiley.com/erras-ad-conditions) on Wiley Online Library for rules of use; OA articles are

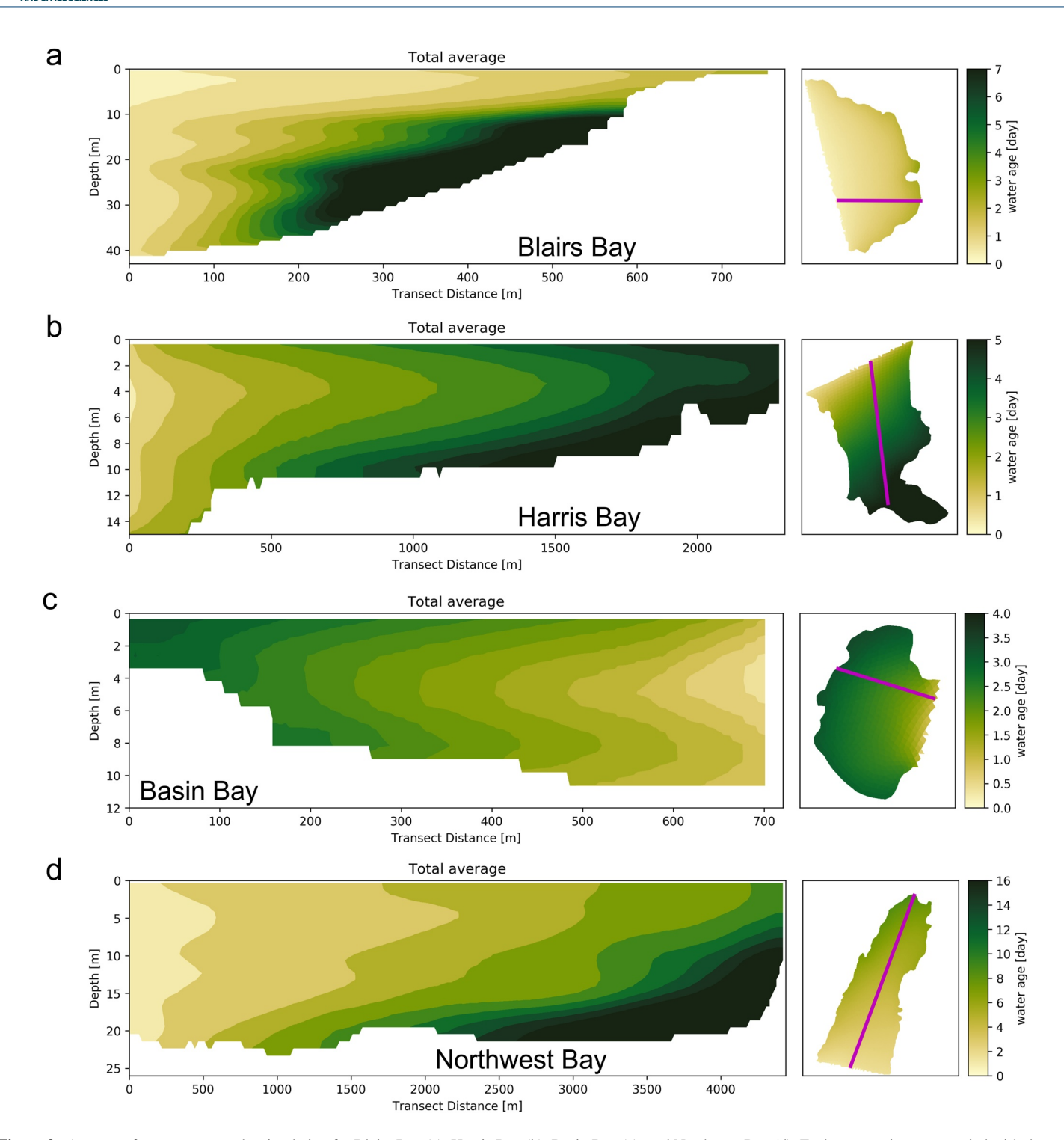


Figure 9. Average of water age over the simulation for Blairs Bay (a), Harris Bay (b), Basin Bay (c), and Northwest Bay (d). Each transect is accompanied with the temporally averaged water age at the surface and the location of the transect (magenta line).

Our simulation results suggest that at the daily timescale, a substantial portion of the water in the bay can be transported into the main body of the lake, along with the constituents suspended in the water.

Volume averages mask the complex spatial distribution of water age in the bays. The averaged transects demonstrate that the vertical distribution is far from uniform, with portions of the water volumes remaining for longer periods of time, sometimes more than 1 week (Northwest Bay and Blairs Bay) whereas other water parcels within

AUGER ET AL. 15 of 17

19447973, 2024, 2, Downloaded

1029/2022WR034168 by Rensselaer Polytechnic

Acknowledgments

We gratefully acknowledge assistance by

personnel associated with the Jefferson

Project at Lake George, a collaboration

IBM Research and the Lake George

between Rensselaer Polytechnic Institute,

Association. In addition to funding from

the three partners, the sensor network has

been partially supported by a NSF MRI

Grant (#1655168) and a New York State

Higher Education Capital Grant (#7290).

KCR was also supported by NSF Grants

1754265 and 2048031. We acknowledge

the great help from Brian Mattes from

the Darrin Fresh Water Institute in the

deployment of the vertical profilers. We

also would like to thank the anonymous

comments that substantially improved our

reviewers who provided constructive

manuscript for publication.

the same bay have a water age less than 2.5 days. The older portion of water usually exists in a 5 m-thick layer above the bottom closer to the head of the bay. At the mouth of the bays, water is repeatedly mixed with water from the main basin within 24 hr, suggesting a transfer of suspended material into the main basin in the same time frame. Snapshots of water age transects indicated that strong wind events substantially change the vertical distribution of water age in some of the bays, even to the point of inverting the distribution. However, strong wind events can have small impacts on the vertical distribution of water age in deep bays.

To obtain the numerical results described in the present article, we used a high-resolution bathymetry to resolve some of the complex smaller bays and their currents. Because of the cost, high-resolution bathymetric surveys are rare and lower resolution bathymetry data sets are typically used in hydrodynamic simulations. Given the dependency on the bathymetry, future work should investigate whether low-resolution bathymetric surveys are sufficient to estimate the residence time in bays of a lake.

#### **Data Availability Statement**

Scripts and data used for the article are available in G. Auger et al. (2023).

#### References

- Auger, G. A. R., Kelly, M. R., Moriarty, V. W., Rose, K. C., & Kolar, H. R. (2023). Understanding lake residence time across spatial and temporal scales: A modeling analysis of Lake George, New York USA [Dataset]. https://doi.org/10.6084/m9.figshare.23979138.v1
- Auger, G. A. R., Watson, C. D., & Kolar, H. R. (2021). The influence of weather forecast resolution on the circulation of Lake George, NY. Water Resources Research, 57(10), e2020WR029552. https://doi.org/10.1029/2020WR029552
- Brooks, J. R., Gibson, J. J., Birks, S. J., Weber, M. H., Rodecap, K. D., & Stoddard, J. L. (2014). Stable isotope estimates of evaporation: Inflow and water residence time for lakes across the United States as a tool for national lake water quality assessments. *Limnology and Oceanography*, 59(6), 2150–2165. https://doi.org/10.4319/jo.2014.59.6.2150
- Deleersnijder, E., Campin, J.-M., & Delhez, E. J. M. (2001). The concept of age in marine modelling I. Theory and preliminary model results. Delhez, E. J. M., Campin, J.-M., Hirst, A. C., & Deleersnijder, E. (1999). Toward a general theory of the age in ocean modelling. *Ocean Modelling*, *I*(1), 17–27. https://doi.org/10.1016/S1463-5003(99)00003-7
- Doda, T., Ramón, C. L., Ulloa, H. N., Wüest, A., & Bouffard, D. (2022). Seasonality of density currents induced by differential cooling. Hydrology and Earth System Sciences, 26(2), 331–353. https://doi.org/10.5194/hess-26-331-2022
- Duffy, C. J., Dugan, H. A., & Hanson, P. C. (2018). The age of water and carbon in lake-catchments: A simple dynamical model. *Limnology and Oceanography Letters*, 3(3), 236–245. https://doi.org/10.1002/iol2.10070
- Evans, C. D., Futter, M. N., Moldan, F., Valinia, S., Frogbrook, Z., & Kothawala, D. N. (2017). Variability in organic carbon reactivity across lake residence time and trophic gradients. *Nature Geoscience*, 10(11), 832–835. https://doi.org/10.1038/ngeo3051
- Fairall, C. W., Bradley, E. F., Hare, J. E., Grachev, A. A., & Edson, J. B. (2003). Bulk parameterization of air–sea fluxes: Updates and verification for the COARE algorithm. *Journal of Climate*, 16(4), 571–591. https://doi.org/10.1175/1520-0442(2003)016<0571:BPOASF>2.0.CO;2
- Fergus, C. E., Brooks, J. R., Kaufmann, P. R., Herlihy, A. T., Pollard, A. I., Weber, M. H., & Paulsen, S. G. (2020). Lake water levels and associated hydrologic characteristics in the conterminous U.S. *JAWRA Journal of the American Water Resources Association*, 56(3), 450–471. https://doi.org/10.1111/1752-1688.12817
- Fringer, O. B., Gerritsen, M., & Street, R. L. (2006). An unstructured-grid, finite-volume, nonhydrostatic, parallel coastal ocean simulator. *Ocean Modelling*, 14(3–4), 139–173. https://doi.org/10.1016/j.ocemod.2006.03.006
- Gelda, R. K., King, A. T., Effler, S. W., Schweitzer, S. A., & Cowen, E. A. (2015). Testing and application of a two-dimensional hydrothermal/transport model for a long, deep, and narrow lake with moderate Burger number. *Inland Waters*, 5(4), 387–402. https://doi.org/10.5268/IW-5.4.804
- Hintz, W. D., Schuler, M. S., Borrelli, J. J., Eichler, L. W., Stoler, A. B., Moriarty, V. W., et al. (2020). Concurrent improvement and deterioration of epilimnetic water quality in an oligotrophic lake over 37 years. *Limnology and Oceanography*, 65(5), 927–938. https://doi.org/10.1002/lno.11359
- Li, Y., Acharya, K., Chen, D., & Stone, M. (2010). Modeling water ages and thermal structure of Lake Mead under changing water levels. Lake and Reservoir Management, 26(4), 258–272. https://doi.org/10.1080/07438141.2010.541326
- Liu, S., Ye, Q., Wu, S., & Stive, M. J. F. (2020). Wind effects on the water age in a large shallow lake. Water, 12(5), 1246. https://doi.org/10.3390/wi12051246
- Marsh, G. A., & Fairbridge, R. W. (1999). Lentic and lotic ecosystems. In *Environmental geology* (pp. 381–388). Kluwer Academic Publishers. https://doi.org/10.1007/1-4020-4494-1\_204
- Michalak, A. M., Anderson, E. J., Beletsky, D., Boland, S., Bosch, N. S., Bridgeman, T. B., et al. (2013). Record-setting algal bloom in Lake Erie caused by agricultural and meteorological trends consistent with expected future conditions. *Proceedings of the National Academy of Sciences*, 110(16), 6448–6452. https://doi.org/10.1073/pnas.1216006110
- NYDEC. (2022). Harmful algal bloom action plan Lake George. Retrieved from https://lgpc.ny.gov/system/files/documents/2022/09/lg-hab-plan-2022-update.pdf
- Rayson, M. D., Gross, E. S., Hetland, R. D., & Fringer, O. B. (2016). Time scales in Galveston Bay: An unsteady estuary. *Journal of Geophysical Research: Oceans*, 121(4), 2268–2285. https://doi.org/10.1002/2015JC011181
- Rose, K. C., Graves, R. A., Hansen, W. D., Harvey, B. J., Qiu, J., Wood, S. A., et al. (2017). Historical foundations and future directions in macrosystems ecology. *Ecology Letters*, 20(2), 147–157. https://doi.org/10.1111/ele.12717
- Rueda, F. J., & Cowen, E. A. (2005). Residence time of a freshwater embayment connected to a large lake. Limnology and Oceanography, 50(5), 1638–1653. https://doi.org/10.4319/lo.2005.50.5.1638
- Rueda, F. J., Schladow, S. G., & Clark, J. F. (2008). Mechanisms of contaminant transport in a multi-basin lake. *Ecological Applications*, 18(sp8), A72–A88. https://doi.org/10.1890/06-1617.1

AUGER ET AL. 16 of 17



## **Water Resources Research**

10.1029/2022WR034168

Shuster, E. L., LaFleur, R. G., & Boylen, C. W. (1994). The hydrologic budget of Lake George, Southeastern Adirondack Mountains of New York. Northeastern Geology, 16, 94–108.

Swinton, M. W., & Boylen, C. W. (2014). Phytoplankton and macrophyte response to increased phosphorus availability enhanced by rainfall quantity. *Northeastern Naturalist*, 21(2), 234–246. https://doi.org/10.1656/045.021.0204

Zhao, F., Zhan, X., Xu, H., Zhu, G., Zou, W., Zhu, M., et al. (2022). New insights into eutrophication management: Importance of temperature and water residence time. *Journal of Environmental Sciences*, 111, 229–239. https://doi.org/10.1016/j.jes.2021.02.033

AUGER ET AL. 17 of 17